

## DEPENDENCE BETWEEN CALCULATED FLEXIBILITY OF LAMELLAS OF LAYERED MATERIALS AND THEIR ABILITY TO UNDERGO INTERCALATION REACTIONS

Jiří VOTINSKÝ<sup>a</sup> and Ludvík BENĚŠ<sup>b</sup>

<sup>a</sup> Department of General and Inorganic Chemistry,  
Institute of Chemical Technology, 532 10 Pardubice

<sup>b</sup> Joint Laboratory of Solid State Chemistry of Czechoslovak  
Academy of Sciences and Institute of Chemical Technology, 532 10 Pardubice

Received February 6, 1991

Accepted March 20, 1991

A computational procedure has been suggested enabling estimates of the flexibility of individual layers of layered materials from their crystallographical structure. The data about flexibility of layers have been obtained by calculation for compounds of the type  $Q_2Y_3$  ( $Q = Sb^{III}, Bi^{III}, Y = Se^{-II}, Te^{-II}$ ; space group of symmetry  $R\bar{3}m$ ),  $MPS_3$  ( $M = Mn^{II}, Fe^{II}, Co^{II}, Ni^{II}, Cd^{II}, C2/m$ ),  $TX_2$  ( $T = Nb^{IV}, Ta^{IV}, Mo^V$ ;  $X = S^{-II}, Se^{-II}$ ;  $P6_3/mmc$ ),  $FeOCl$  ( $Pnmm$ ),  $Zr(HPO_4)_2$  ( $P2_1/n$ ) and  $ROPO_4$  ( $R = V^V, Nb^V, Mo$ ;  $P4/n$ ). The flexibility of the layers of these compounds increases in the order:  $Q_2Y_3 \lll MPS_3 < TX_2 < FeOCl = Zr(HPO_4)_2 < ROPO_4$ . The same trend is observed for the ability of these compounds to form intercalates. In most of the structures given a distinct anisotropy of flexibility has been found by the calculation.

If we try to intuitively suggest mechanisms by which large particles such as molecules of aliphatic amines, alcohols, carboxylic acids, metallocenes, pyridine, etc. could enter between layers of a host during intercalation reactions, we cannot avoid the presumption that in the reaction zone the host layers are bent. For illustration two such mechanisms suggested by us are given in Fig. 1, their principle being obvious from the scheme.

In both the mechanisms it is considered likely that the entering of guest molecules is started by rising and bending of the first surface layer of the host. Immediately afterwards the molecules begin to penetrate below the next layer and the process continues. It is not presumed that the intercalation process and opening of the host layers might start at another place of the microcrystal. Mechanism *A* involves a simple bending of layers, the layers being bent only in the area of the reaction zone. In mechanism *B* a multiple bending occurs, the flexures being maintained in the structure of the layered complex formed until the intercalation is finished. Whereas in mechanism *A* the penetration of the guest molecules between the host layers will not stop once started, in mechanism *B* the entering of molecules into one interlayer area temporarily blocks the penetration of molecules into the neighbouring

interlayers. Hence by mechanism B an easy formation of the so-called stages<sup>1-3</sup> would also be possible for molecular intercalates. The structure of some layered complexes can be derived from that of the host by mere opening of the layers, or alternatively the opening is accompanied by a tangential shift of the layers by a fraction of the layer structure motif. Both mechanisms not only allow, but even necessitate, such sliding of layers.

It cannot be decided whether or not some of the mechanisms suggested or another mechanism of similar type are real, nor is it possible to find it experimentally. Hence we tried to verify – at least indirectly and qualitatively – that it is justified to presume that the bending of host layers represents a component part of the real mechanism. The verification was based on a simple idea: If the intercalation involves bending of the host layers and if the energy needed for formation of bending contributes to the activation energy of intercalation, then a material whose layers are more flexible must intercalate more easily under comparable conditions (i.e. more rapidly and at lower temperatures).

However, no data are available in the literature about the rigidity of the host layers. Therefore, we have suggested a simple calculation enabling the estimation of the rigidity of a layer from its crystallographical structure.

The calculation has been applied to an extensive group of layered materials and its results have been compared with the experimental data about the tendency of these compounds towards formation of intercalates with molecular species.

### CALCULATIONS

The calculation is based on a simplifying presumption that the rigidity of a layer is proportional to the overall lengthening or shortening of the bonds present per a layer surface unit which occurs during bending of the layer in a definite, precisely specified way. The calculation neglects the fact that the contribution of each bond to the mechanical strength of the layer also depends on the force constant of that bond.

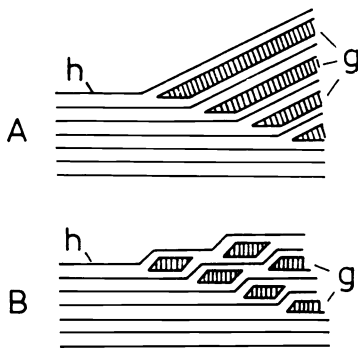


FIG. 1

Two intuitively suggested mechanisms for molecules entering a host layered structure (g host, h guest)

The calculation involves a balance of the smallest structural motif whose translation in the plane produces the layer. The dimensions of the parallelepiped circumscribed to this structural motif are  $a$ ,  $b$  and  $c$ . The parallelepiped has identical dimensions with those of the elementary host cell, provided the cell contains a single layer. If the elementary cell involves several layers, then the parallelepiped forms a part of the cell.

The sum  $L$  of the lengths of all bonds inside the parallelepiped is given by the relation (1),

$$L = \sum_i l_i v_i, \quad (1)$$

where  $l_i$  denotes the length of the  $i$ -th bond, and  $v_i$  stands for the matrix element characterizing the bond.

The length  $l_i$  of a bond connecting two atoms with the coordinates  $x_n, y_n, z_n$  and  $x_p, y_p, z_p$  is given by Eq. (2).

$$l_i = [(x_n - x_p)^2 + (y_n - y_p)^2 + (z_n - z_p)^2]^{1/2} \quad (2)$$

The matrix element has the value  $v_i = 1$  if the whole  $i$ -th bond lies inside the parallelepiped. If it extends into two or four parallelepipeds, then it is  $v_i = 1/2$  or  $1/4$ , respectively. If no bond exists between two particular atoms, then it is viewed as having  $v_i = 0$ .

Two geometrically different ways of layer bending were chosen for the calculation: they are represented schematically in Fig. 2.

In the first way of bending the structural motif is bent such that if the deformation force changed its direction continuously throughout the bending it would be always and everywhere perpendicular to the layer bent. The set of planes,  $x = k$  ( $0 \leq k \leq a$ ) which are parallel in the structural motif before the bending mutually intersect in the bending axis  $o$  ( $o \parallel y$ ) after the bending.

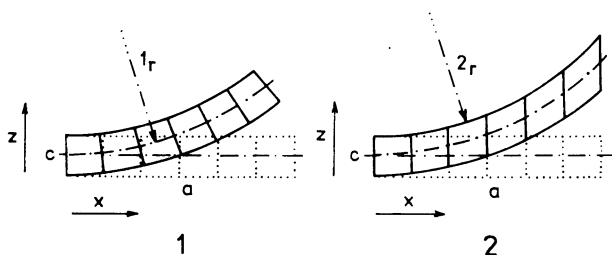


FIG. 2

Two ways of bending of host layer: 1 the bending deformation produced by action of a directionally variable force perpendicular to the layer; 2 shear deformation of the layer by two opposite parallel forces of constant direction

The second way of bending of the structural motif resembles a deformation caused by a shear force. The planes  $x = k$  remain parallel during this way of bending.

The length  ${}^1l_i$  of the  $i$ -th bond after the bending in the first way is given by Eq. (3).

$${}^1l_i = [({}^1r - z_n)^2 + ({}^1r - z_p)^2 - 2({}^1r - z_p) \cos(180(x_n - x_p)/80) + (y_n - y_p)^2]^{1/2}, \quad (3)$$

where  ${}^1r$  means the radius of curvature of the bending of the plane  $z = c/2$ . For the radius of curvature we chose the value:

$${}^1r = 80/\pi + c/2. \quad (4)$$

In the second way of bending the new length  ${}^2l_i$  of the  $i$ -th bond is given by Eq. (5)

$${}^2l_i = \{[l_i - (z_n - z_p)^2 + z_n - z_p + ({}^2r^2 - x_p)^{1/2} - ({}^2r^2 - x_n^2)^{1/2}]^2\}^{1/2} \quad (5)$$

The radius of curvature  ${}^2r$  of any of the bent planes  $z = k$  ( $0 \leq k \leq c$ ) was chosen as:

$${}^2r = 80/\pi. \quad (6)$$

It can be expected that the flexibility of a structural motif of a layer will be the smaller the greater the number of bonds in the motif which undergo lengthening or shortening during the bending and the greater this lengthening or shortening. This means that a motif is the more rigid the greater is the sum of absolute values of differences of bonds lengths before and after the bending carried out in the first or second way. These sums  $\Delta^1L$  and  $\Delta^2L$  are given in Eqs (7a,b).

$$\Delta^1L = \sum_i v_i (|l_i - {}^1l_i|) \quad \Delta^2L = \sum_i v_i (|l_i - {}^2l_i|) \quad (7a, b)$$

In order to obtain comparable results from the calculations carried out for various layered structures, it is useful to divide the values  $\Delta^1L$  and  $\Delta^2L$  by the surface area  $P = ab$  of the base of the parallelepiped. Thus we obtain sums of absolute values of bond length changes during bending of the motif related to a surface unit:

$${}^1S = \Delta^1L/P \quad {}^2S = \Delta^2L/P. \quad (8a, b)$$

It follows from Fig. 2 that in the calculations we chose such a position of the structural motif in the coordinate system for which it is  $a \parallel x$  and  $b \parallel y$ . The orientation of the bending axis  $o$  is determined by the condition  $o \parallel y$ . The angle  $\varphi$  formed by the bending axis  $o$  and the  $x$  axis of the coordinate system is  $90^\circ$ . This position of the

structural motif within the coordinate system can be denoted as special. Simple transformation of coordinates can be used to simulate rotation of the structural motif in the plane of the  $x$  and  $y$  axes around the  $z$  axis whereby the angle  $\varphi$  is changed. A particular geometry of dislocation of atoms and bonds within the structural motif can make itself felt by an anisotropy of the quantities  $^1S$  and  $^2S$  depending on the  $\varphi$  angle varied. The calculation thus enables us to find the directions in which the structural motif, and hence also the layer exhibit the lowest or — on the contrary — the highest flexibility.

The extreme values of the quantity  $S$  were sought on the basis of the condition  $dS/d\varphi = 0$  in the courses of the calculated function  $S = f(\varphi)$  within the interval  $0^\circ \leq \varphi \leq 180^\circ$ . The extremes found are denoted as  $S_{\min}$  and  $S_{\max}$  and the respective angles as  $\varphi_{\min}$  and  $\varphi_{\max}$ .

The calculations started from the data published about the crystallographical structures of the hosts. The calculations according to Eqs (1) through (8) were carried out without any further simplifying presumptions.

## RESULTS

The dependences of the quantities  $^1S$  and  $^2S$  upon  $\varphi$ , calculated for the structures of all the layered hosts analyzed, are presented in Figs 3 and 4. In the cases where —

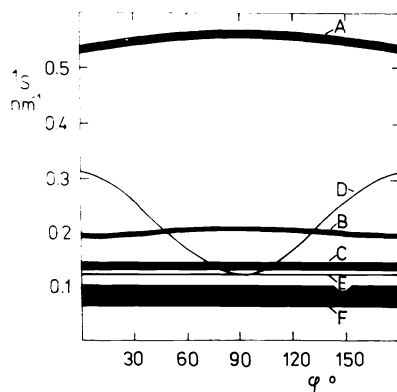


FIG. 3

Dependence of calculated  $^1S$  quantities upon  $\varphi$  angle for the structures: A  $Q_2Y_3$  ( $Q = \text{Sb}^{\text{III}}, \text{Bi}^{\text{III}}; Y = \text{Se}^{-\text{II}}, \text{Te}^{-\text{II}}$ ); B  $\text{MPS}_3$  ( $M = \text{Mn}^{\text{II}}, \text{Fe}^{\text{II}}, \text{Co}^{\text{II}}, \text{Ni}^{\text{II}}, \text{Cd}^{\text{II}}$ ); C  $\text{TX}_2$  ( $T = \text{Nb}^{\text{IV}}, \text{Ta}^{\text{IV}}, \text{Mo}^{\text{IV}}; X = \text{S}^{-\text{II}}, \text{Se}^{-\text{II}}$ ); D  $\text{FeOCl}$ ; E  $\text{Zr}(\text{HPO}_4)_2$ ; F  $\text{ROPO}_4$  ( $R = \text{V}^{\text{V}}, \text{Nb}^{\text{V}}, \text{Mo}^{\text{V}}$ )

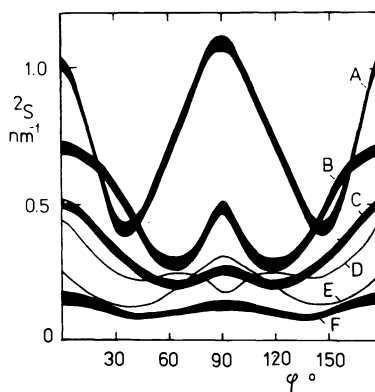


FIG. 4

Dependences of calculated  $^2S$  quantities upon  $\varphi$  angle for the structures examined. For the meaning of symbols A—F see Fig. 3

for groups of isostructural compounds – those curves are of identical shape and only slightly mutually shifted, they are represented as hatched bands.

Table I gives the calculated extremes of the quantities  $^1S$  and  $^2S$  and the cor-

TABLE I  
The extreme values of  $^1S$  and  $^2S$  quantities found for the angles from the interval  $0^\circ \leq \varphi \leq 180^\circ$

Host	Space group (references)	$^1S_{\min}, \text{nm}^{-1}$ ( $\varphi_{\min}, ^\circ$ )	$^1S_{\max}, \text{nm}^{-1}$ ( $\varphi_{\max}, ^\circ$ )	$^2S_{\min}, \text{nm}^{-1}$ ( $\varphi_{\min}, ^\circ$ )	$^2S_{\max}, \text{nm}^{-1}$ ( $\varphi_{\max}, ^\circ$ )
VOPO <sub>4</sub>		<sup>a</sup> 0.072		0.100	0.155
				(50, 130)	(0, 180)
MoOPO <sub>4</sub>	<i>P4/n</i> (6, 7)	<sup>a</sup> 0.090		0.089	0.176
				(45, 135)	(0, 180)
NbOPO <sub>4</sub>		<sup>a</sup> 0.092		0.082	0.159
				(45, 135)	(0, 180)
Zr(HPO <sub>4</sub> ) <sub>2</sub>	<i>P2<sub>1</sub>/n</i> (4)	<sup>a</sup> 0.134		0.122	0.312
FeOCl	<i>Pmm</i> (5)	0.123 (90)	0.319 (0, 180)	0.176	0.435
				0.230 (42, 138)	0.247 (67, 113)
NbS <sub>2</sub>		<sup>a</sup> 0.139		0.209	0.514
				(58, 122)	(0, 180)
NbSe <sub>2</sub>	<i>P6<sub>3</sub>/mmc</i> (11–13)	<sup>a</sup> 0.141		0.211	0.520
				(58, 122)	(0, 180)
TaSe <sub>2</sub>		<sup>a</sup> 0.141		0.213	0.524
				(58, 122)	(0, 180)
MoS <sub>2</sub>		<sup>a</sup> 0.146		0.229	0.539
				(58, 122)	(0, 180)
				0.284 (90)	0.293 (90)

TABLE I  
 (Continued)

Host	Space group (references)	$^1S_{\min}, \text{nm}^{-1}$ ( $\varphi_{\min}, ^\circ$ )	$^1S_{\max}, \text{nm}^{-1}$ ( $\varphi_{\max}, ^\circ$ )	$^2S_{\min}, \text{nm}^{-1}$ ( $\varphi_{\min}, ^\circ$ )	$^2S_{\max}, \text{nm}^{-1}$ ( $\varphi_{\max}, ^\circ$ )
MnPS <sub>3</sub>		0.193	0.208	0.275	0.703
		(0, 180)	(90)	(62, 118)	(0, 180)
FePS <sub>3</sub>		0.195	0.209	0.258	0.498
		(0, 180)	(90)	(62, 118)	(90)
CoPS <sub>3</sub>	C2/n (8)	0.196	0.210	0.254	0.707
		(0, 180)	(90)	(62, 118)	(0, 180)
NiPS <sub>3</sub>		0.196	0.210	0.260	0.504
		(0, 180)	(90)	(62, 118)	(90)
CdPS <sub>3</sub>		0.191	0.205	0.255	0.711
		(0, 180)	(90)	(62, 118)	(0, 180)
Bi <sub>2</sub> Se <sub>3</sub>	R3m (9–10)	0.541	0.564	0.428	0.506
		(0, 180)	(90)	(33, 147)	(90)
Sb <sub>2</sub> Te <sub>3</sub>		0.540	0.563	0.424	0.698
		(0, 180)	(90)	(33, 147)	(0, 180)
					0.497
					(90)
					1.125
					(90)
					1.080
					(0, 180)
					1.117
					(90)
					1.071
					(0, 180)

<sup>a</sup>  $^1S$  - const. (for the all  $\varphi$  values).

responding angles. Its first column gives the formulas of hosts, the space group and citations of papers from which the data on the crystallographical structure were taken. Isostructural compounds form individual groups in this table. The second and the third columns of this Table present the values  $^1S_{\min}$  and  $^1S_{\max}$  and the respective angles  $\varphi_{\min}$  and  $\varphi_{\max}$ . When using the first way of bending, some structures exhibit constant  $^1S$  which is independent of  $\varphi$  (see Fig. 3). In these cases the calculated  $^1S$  values are given in the middle space between the columns 2 and 3 of

the table. The last two columns presenting the extreme values of the  ${}^2S$  quantity are arranged in similar way.

Table II shows the sequence of host structures obtained if they were arranged according to the  ${}^1S_{\max}$ ,  ${}^1S_{\min}$ ,  ${}^2S_{\max}$ ,  ${}^2S_{\min}$  values found by the calculation. The host with the largest value of sum of bond length changes stands on the 1st position whereas the host with the least change occupies the 6th position.

## DISCUSSION

From Table II it follows that the order of hosts arranged according to the calculated rigidity of their layers on the basis of the  ${}^1S_{\min}$  and  ${}^3S_{\min}$  values is expressed by the following sequence for both the ways of bending used:



(The symbols used in the formulas have the following meaning: Q = Sb, Bi; Y = Se, Te; M = Mn, Fe, Co, Ni, Cd; T = Nb, Ta, Mo; X = S, Se; R = V, Nb, Mo).

It is interesting to compare this qualitative sequence with available experimental findings about the intercalation of these compounds. The compounds of  $Q_2Y_3$  type ( $R3m$ ), which exhibit the highest rigidity according to the calculation, have not yet been successfully intercalated with molecular species. The hosts of the type  $MPS_3$  ( $C2/m$ ) and  $TX_2$  ( $P6_3/mmc$ ) accept pyridine molecules only after a several day contact with the liquid at temperatures in the range from 80 to 200°C (refs<sup>14-16</sup>).  $FeOCl$  ( $Pmnm$ ) intercalates pyridine at temperatures of 50–80°C (refs<sup>17-19</sup>) and  $Zr(HPO_4)_2$  ( $P2_1/n$ ) rapidly forms a layered complex with pyridine at room temperature (ref.<sup>20</sup>).

TABLE II

The order of rigidity of layers of the structures examined arranged according to the extreme values of  ${}^1S_{\max}$ ,  ${}^1S_{\min}$ ,  ${}^2S_{\max}$ ,  ${}^2S_{\min}$  ( $\text{nm}^{-1}$ )

Host	${}^1S_{\max}$	${}^1S_{\min}$	${}^2S_{\max}$	${}^2S_{\min}$
$Q_2Y_3$	1	1	1	1
$MPS_3$	3	2	2	2
$TX_2$	4	3	3	3
$FeOCl$	2	5	4	4
$Zr(HPO_4)_2$	5	4	5	5
$ROPO_4$	6	6	6	6



Similar results are obtained also from the reactions of the hosts with aliphatic and aromatic amines, metallocenes, carboxylic acids, alcohols, and some other compounds. Whereas for the  $\text{MPS}_3$  and  $\text{TX}_2$  hosts typical syntheses last several days or even weeks at 120–200°C, the intercalations of  $\text{FeOCl}$  are completed within much shorter reaction times at 30–100°C.  $\text{Zr}(\text{HPO}_4)_2$  accepts foreign molecules between its layers at room temperature in most cases. The layered phosphates of general formula  $\text{ROPO}_4$  and vanadyl(IV)sulfate ( $P4/n$ ) – according to our findings – accept aliphatic alcohols at room temperature within several minutes, and the systems must be heated only in the cases of higher alcohols<sup>21,22</sup>.

Obviously the data on temperatures used in the syntheses are not identical with the threshold temperatures for the start of intercalation. Nevertheless it can be presumed that the temperature of syntheses to a certain extent reflect the tendency of hosts to intercalate and are connected with the activation energies of the reactions. If we accept this presumption we must admit that the host layer bending could form a part of the intercalation process.

Moreover the results of our simple calculations show that the flexibility of layers can exhibit anisotropy. As a consequence, it is possible that the reaction zones in the intercalation processes of layered hosts spread only in certain preferred directions in the crystals.

In compounds of the type  $\text{MPS}_3$  the layer bending should shift on the layer along four crystallographically equivalent directions  $\langle 100 \rangle$ . On the layers of  $\text{Zr}(\text{HPO}_4)_2$  and  $\text{ROPO}_4$  the reaction zones should move along the directions  $\langle 210 \rangle$  and  $\langle 110 \rangle$ . The denotation of directions is in accordance with the coordinate systems defined for the structures given in the reports cited in Table I.

## REFERENCES

1. Clarke R., Uher C.: *Adv. Phys.* **33**, 469 (1984).
2. Kirczenow G.: *Can. J. Phys.* **66**, 39 (1988).
3. Whittingham M. S., Jacobson A. J. (Eds): *Intercalation Chemistry*. Academic Press, New York 1982.
4. Troup J. M., Clearfield A.: *Inorg. Chem.* **16**, 3311 (1977).
5. Palvadeau P., Venien J. P., Calvarin G.: *C. R. Acad. Sci.*, **2** 292, 1259 (1981).
6. Tachez M., Theobald F., Bernard J., Hewat A. W.: *Rev. Chim. Miner.* **19**, 291 (1982).
7. Jordan B., Calvo C.: *Acta Crystallogr.*, **B** **32**, 2899 (1976).
8. Ouvrad G., Brec R., J. Rouxel: *Mat. Res. Bull.* **20**, 1181 (1985).
9. Donges E.: *Z. Anorg. Allg. Chem.* **265**, 56 (1951).
10. Lange P. W.: *Naturwissenschaften* **27**, 133 (1939).
11. Kadijk F., Huisman R. G., Jellinek F.: *Recueil* **83**, 768 (1964).
12. Jellinek F., Brawer G., Müller H.: *Nature* **185**, 376 (1960).
13. Dickinson R. G., Pauling L.: *J. Am. Chem. Soc.* **45**, 1464 (1923).
14. Fuita O., Aoki R.: *Synth. Met.* **6**, 111 (1983).
15. Nakamura S., Aoki R.: *Synth. Met.* **6**, 201 (1983).

16. Hamane Y., Aoki R.: *J. Phys. Soc. Jpn.* *55*, 1327 (1986).
17. Herber R. H., Maeda Y.: *Inorg. Chem.* *20*, 1409 (1981).
18. Salmon A., Eckert H., Herber R. H.: *J. Chem. Phys.* *81*, 5206 (1984).
19. Rouxel J., Palvadeau P.: *Rev. Chem. Miner.* *19*, 317 (1982).
20. Kijima T., Goto M.: *Thermochim. Acta* *63*, 33 (1983).
21. Beneš L., Votinský J., Kalousová J., Klikorka J.: *Inorg. Chim. Acta* *114*, 47 (1986).
22. Votinský J., Beneš L., Kalousová J., Klikorka J.: *Inorg. Chim. Acta* *126*, 19 (1987).

Translated by J. Panchartek.